A Remote Sensing Approach to Identifying Drought Onset and Progression in Central India

Hempushpa Sahu [1], Pradeep Kumar Garg [2], Saurabh Vijay [3]

[1] Research Scholar, Geospatial Group, Department of Civil Engineering, IIT Roorkee, India- hempushpa09@gmail.com
[2] Emeritus Professor, Geospatial Group, Department of Civil Engineering, IIT Roorkee, India- p.garg@ce.iitr.ac.in
[3] Geospatial Group, Department of Civil Engineering, IIT Roorkee, India- saurabh.vijay@ce.iitr.ac.in

Keywords: Drought, Bundelkhand, ERA5- Land, GIMMS NDVI, CHIRPS

Abstract

Climate change is intensifying the frequency and severity of droughts, making it important to understand their impacts on ecosystems and society. However, to analyse the relationship between the main sources of agriculture drought is always challenging. The development of remote sensing technology, provides diverse datasets at varying spatial and temporal resolutions, making drought assessment and monitoring comparatively easier than previous time. This study aims to evaluate the effectiveness of multisource remote sensing data in monitoring agricultural drought conditions in the Bundelkhand region. The datasets used are CHIRPS, ERA5 Land, and PKU GIMMS NDVI to derive four drought indices: the Standardized Precipitation Index (SPI), the Rainfall Anomaly Index (RAI), Soil Moisture Condition Index (SMCI), and Vegetation Condition Index (VCI). In addition, we also performed pixel wise Pearson correlation analysis to examine relationships among these indices, resulting in a correlation from 0.25 to 0.7 between SMCI and VCI. The rainfall and soil moisture relation was found to be 0.294 between RAI and SMCI, but vegetation response is well observed with SPI 3 and VCI at 0.492, indicating their lagged relationship. Monthly variation analysis indicated that June experienced the lowest vegetation activity, while September exhibited both soil moisture and vegetation stress, indicating drought development across the monsoon season. The analysis of 2015 showed the rainfall anomalies and vegetation response are highly interrelated, validating drought in the year. The paper highlights the importance of remote sensing for drought assessment and supplementing its importance for disaster management and mitigation implementations.

1. Introduction

Drought is a complex, slow occurring phenomenon that is an internal part of the climate cycle. It is one of the costliest natural disasters (Zhao et al., 2021). Its complex nature is due to gradual development and non-structural damage thus making it difficult to detect and understand. And thus, it requires, a different strategies of planning, preparedness and management (Mahmoudi et al., 2019). The definition of drought in simple words is described as a period of prolonged precipitation deficit. Droughts are commonly classified into four types: meteorological drought, due to reduced precipitation; agricultural drought, due to insufficient soil moisture and a reduced crop yields; hydrological drought, when a reduction in reservoirs, rivers, and lakes is observed; and socio-economic drought, which occurs when demand exceeds supply. Drought is not governed by a single variable but by multiple interrelated variables, such as precipitation, soil moisture, humidity, temperature, evapotranspiration, and various climate indices, which together contribute to its complexity and makes it challenging.

Earlier, meteorological variables were collected from ground-based observation stations. But, with the advent of technology, satellite data are available with these variables, which reduce the barrier of spatio-temporal resolutions. Different drought indices have been developed so far, with different variables for understanding droughts. Studies using these indices were dependent on station based datasets for analyzing droughts. Mostly used indices include Standardized Precipitation Index (SPI) (Mckee et al., 1993), Rainfall Anomaly Index (RAI) (Van Rooy, 1965), Percent of Normal Index (PNI) (Werick et al., 1994), Z-Score Index, Palmer Drought Severity Index (PDSI) (Palmer, 1965), Standardized Precipitation Evapotranspiration Index (SPEI) (Vicente-Serrano et al., 2010), etc.,. other than these remote sensing based indices as Normalized Difference Vegetation Index (NDVI), Vegetation Condition Index (VCI) (Kogan, 1995), Vegetation Health Index (VHI) (Bhuiyan et al., 2017) are also widely used.

In this regard, some sources of precipitation and soil moisture data are available for drought monitoring are the Climate Hazards Group InfraRed Precipitation with Stations (CHIRPS) (Ocampo-Marulanda et al., 2022), the Tropical Rainfall Measuring Mission (TRMM), and a radar based soil moisture datasets such as Soil Moisture Ocean Salinity (SMOS) and Soil Moisture Active Passive (SMAP) are available for different purposes (Karthikeyan et al., 2020). Other drought related variables including the NDVI, Land Surface Temperature (LST), Evapotranspiration (ET) can be derived from MODIS products. In addition to this, reanalysis data such as ERA5 Land and Global Land Data Assimilation System (GLDAS) developed by integrating satellite observations with ground based measurements, are modelled and available from long past. Besides this free available data, cloud based platforms such as Google Earth Engine (GEE) have simplified data processing and analysis by providing several satellite datasets in it and also processing storage. However, these platforms still comes with some limitations, such as memory exceeds and runtime error for large areas. Some examples of these indices based studies can be referred here (Jiao et al., 2019; Zhang et al., 2017).

Javed et al. (2021) used different drought indices like SPI, SPEI, SSI, Multivariate Standardized Drought Index (MSDI), and VHI anomaly to inspect agricultural drought. A Pearson correlation test was used to access the relationship between these indices. A high correlation of 0.22 to 0.78 was found in the north China between SPEI and VHI anomaly. Liu et al. (2020) also did a correlation testing among the different drought indicator for China and got a correlation of 0.11 to 0.20 from SPEI-1 to SPEI-12 with VCI. Their analysis concluded that from multiple indices

used Precipitation Condition Index (PCI) showed the highest correlation with SPEI-1 suggesting that as it provided more information on drought as a single drought index. A study on Bundelkhand based on SPI, and SPEI shows that more significant number of drying events is observed in timescales of 3 and 6-months. They also showed that region faced moderate drought at a greater area (Gond et al., 2023). Chere & Debalke (2024) studied Ethiopia, for agricultural drought monitoring using SPEI and VHI. The performed monthly correlation analysis from June to September and found that September has highest correlation of 0.74 and August the least. They concluded that SPEI and VHI can be used to detect drought conditions.

In this study, three indices were employed to assess drought conditions: the Standardized Precipitation Index (SPI), and Rainfall Anomaly Index (RAI) representing rainfall, the Soil Moisture Condition Index (SMCI) for soil conditions, and one vegetation representation as Vegetation Condition Index (VCI). The objectives of this paper are: a) to examine the effectiveness of the traditional rainfall based indicator, in identifying drought events; b) to investigate the relationship between soil moisture and vegetation response.

2. Study area

2.1 Study area

India is familiar with the term 'drought' and has faced many incidents in recent decades. One such location is the Bundelkhand region in central India, which lies between 23˚20' to 26˚20' N latitude and 78˚20' to 81˚40' E longitude and is very frequently hit by drought (Amrit et al., 2018; Thomas et al., 2015). Bundelkhand comprises 13 districts, seven from Uttar Pradesh state and six from Madhya Pradesh state. Uttar Pradesh has seven districts Banda, Chitrakoot, Hamirpur, Jalaun, Jhansi, Lalitpur, and Mahoba. This paper analyses the Uttar Pradesh Bundelkhand region, which frequently faces drought (Gupta et al., 2014; Ministry of Agriculture and Farmers Welfare & Government of India, 2022). Figure 1 shows the location of the study area and the annual sum of precipitation for the study period from 2000 to 2021. It has a semi-humid climatic condition and the mean annual rainfall varies from 600 m to 900 mm, mostly received at monsoon period from July to September, and temperature varies from 5˚-10˚ C at winters to high as 35˚- 48˚C in summers (Pandey et al., 2021). The hydrology of the region is it has two main rivers flowing south i.e. Ken and Betwa and other minor tributaries as Pahuj, Dhasan, Tons, Bagahin, and Chambal, and are part of Ganga basin (Thomas et al., 2015). Major population of the region relies on agriculture.

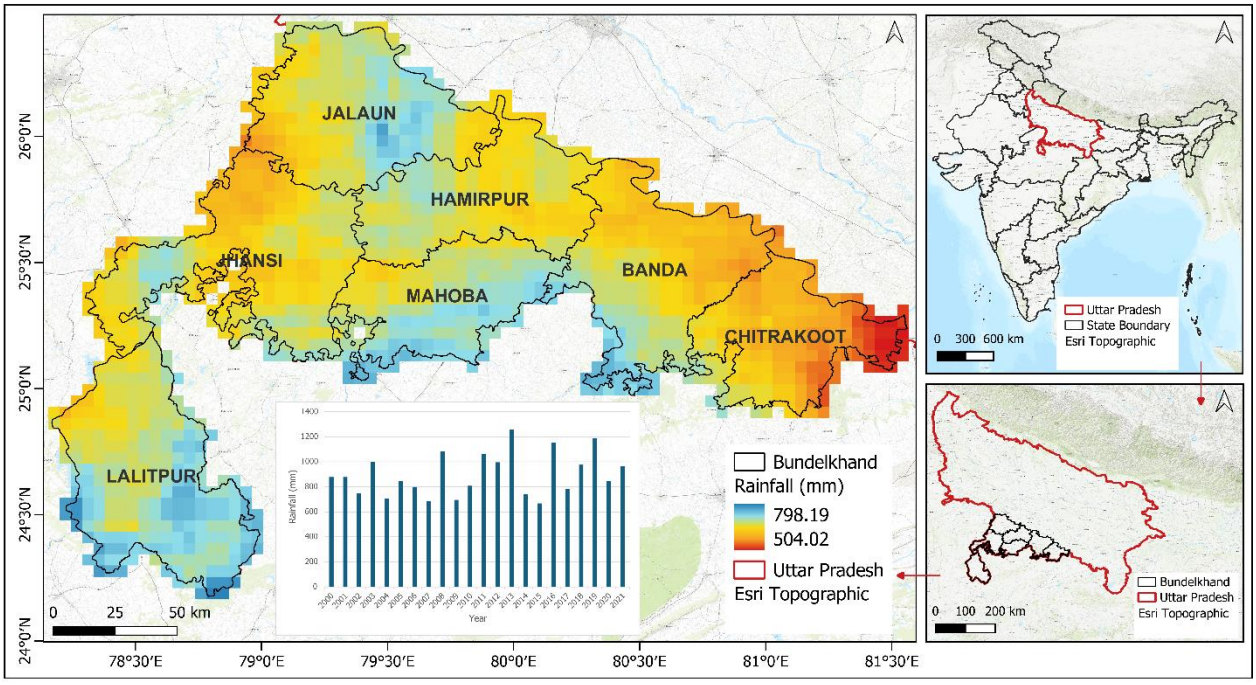

Figure 1. Study area map showing annual mean precipitation of 2015 a drought year. The bar plot shows the annual precipitation of the area from 2000 to 2021.

2.2 Data used

All satellite data used for this work are freely available, and the calculations are done in Google Earth Engine (GEE), R studio, and ArcGIS for further processing. The time for analysis considered is from 2000 to 2021. The CHIRPS satellite precipitation data is a quasi-global (50˚S -50˚N) developed by U.S. Geological Survey (USGS) and the Climate Hazards Group (CHG) of University of California for drought analyzes (Prakash, 2019). It is available at daily and pentad temporal resolution. ERA5- Land is produced by the Copernicus Climate Change Service at the European Centre for Medium-Range Weather Forecasts (ECMWF) is the fifth-generation global reanalysis data and has improved spatial resolution then previous ERA datasets. ERA5-Land used in this study is available from 1950 to present (Vicente-Serrano et al., 2023). Normalized Difference Vegetation Index for Vegetation Condition Index (VCI) is taken from Peking's University Global Inventory Modeling and Mapping Studies (PKU GIMMS) NDVI data which is a consolidated data of Advanced Very High Resolution Radiometer (AVHRR) and Moderate-Resolution Imaging Spectroradiometer (MODIS) NDVI to produce a long term time series data from 1982 to 2022 (Li et al., 2023). The datasets specifications are described in the Table 1.

This contribution has been peer-reviewed. The double-blind peer-review was conducted on the basis of the full paper.
https://doi.org/10.5194/isprs-annals-XI-3-2026-935-2026 | © Author(s) 2026. CC BY 4.0 License.

Table 1. Dataset used in the study

Dataset	Spatial resolution	Temporal resolution	Use
CHIRPS	0.05°	Daily	SPI, RAI
ERA5 -Land	0.1°	Monthly	SMCI
PKU GIMMS	0.0833°	Bi-monthly	VCI

3. Methodology

The calculation of different indices are described in the following sub-sections. As the resolution of all datasets are different, ERA5 Land, has been brought to 8 km, same as GIMMS NDVI resolution using bilinear method. However, using modelled data has their own limitations.

3.1 Standardized Precipitation Index (SPI)

It is calculated using rainfall only and is worldwide used drought indicators, developed by (Mckee et al., 1993). It is derived based on probability using Gamma distribution. SPI can be calculated for different time scales such as 1, 3, 6, 9, 12 months to identify the drought episodes. SPI has been calculated using 'SPEI' package using in R. Detailed explanation can be found in (Dikshit & Pradhan, 2021; Mukhawana et al., 2024). Table 2 shows the classification of each drought index.

3.2 Rainfall Anomaly Index (RAI)

Rainfall Anomaly Index was developed by (Kraus, 1977; Van Rooy, 1965) to identify positive and negative precipitation anomalies over a historical series, it can be calculated on a monthly or annual time scale. It is used to check annual rainfall variability. It is considered to be among the most efficient meteorological indices in terms of result and the simplest in terms of its method of calculation. The RAI considers two anomalies, i.e., positive anomaly and negative anomaly. For this, the precipitation data is arranged in descending order. The first ten highest values are averaged to form a threshold for positive anomaly and the ten lowest values are averaged to form a threshold for negative anomaly. The RAI categorizes humidity/dryness into different classes.

RAI is calculated by the following formula:

$$RAI = 3\left[\frac{P-\bar{P}}{\bar{M}-P}\right] \quad \text{if } P > \bar{P} \quad \ldots\ldots\ldots\ldots\ldots\ldots\ldots\ldots\ldots\ldots (1)$$

$$RAI = -3\left[\frac{P-\bar{P}}{\bar{N}-P}\right] \quad \text{if } P < \bar{P} \quad \ldots\ldots\ldots\ldots\ldots\ldots\ldots\ldots\ldots\ldots (2)$$

Where, P is annual precipitation or the current time precipitation, $\bar{P}$ is the average of the length of record of precipitation available, $\bar{M}$ is the average of the first ten highest precipitation values and $\bar{N}$ is the average of the lowest 10 precipitation values.

3.2 Vegetation Condition Index (VCI)

It is developed by to detect vegetation stress which helps in understanding agricultural drought (Kogan, 1995). Calculated from NDVI it shows the greenness of the region, where high VCI means good vegetation and low means poor vegetation. It varies between 0 to 100 in percentage. It is calculated as shown in equation 3,

$$VCI = 100 * \left(\frac{NDVI - NDVI_{max}}{NDVI_{max} - NDVI_{min}}\right) \quad \ldots\ldots\ldots\ldots\ldots\ldots\ldots\ldots (3)$$

where NDVI is the NDVI value of that time when VCI is to be calculated, and $NDVI_{max}$ and $NDVI_{min}$ are the maximum and minimum NDVI of the period considered.

3.3 Soil Moisture Condition Index (SMCI)

To quantify the soil moisture condition of the region, SMCI was calculated at monthly scale (Lu et al., 2025; Satapathy et al., 2024), given as:

$$SMCI = \frac{SM_i - SM_{i,min}}{SM_{i,max} - SM_{i,min}} \quad \ldots\ldots\ldots\ldots\ldots\ldots\ldots\ldots\ldots\ldots (4)$$

Where, SM_i is the soil moisture of the month, $SM_{i,min}$ and $SM_{i,max}$ are minimum and maximum soil moisture from the time period.

3.4 Pearson Correlation test

A Pearson correlation analysis is conducted between the drought indices to check the degree of correlation between them (Dai et al., 2022). The formula is as follows:

$$R_{xy} = \frac{\sum_{i=1}^{n}(x_i - \bar{x})(y_i - \bar{y})}{\sqrt{\sum_{i=1}^{n}(x_i - \bar{x})^2 \sum_{i=1}^{n}(y_i - \bar{y})^2}} \quad \ldots\ldots\ldots\ldots\ldots\ldots\ldots\ldots (5)$$

Where, x_i and $\bar{x}$, and y_i and $\bar{y}$ are the i-th value and average value of the variable X and Y, respectively. n is the total number of samples sequences. The closer $|R|$ is to 1, the stronger the correlation.

Table 2. Classification of the indices used

RAI	SPI	VCI and SMCI	Category
	SPI > 2.0		Extreme wet
	1.5 ≤ SPI ≤ 1.99		Very wet
	1 ≤ SPI ≤ 1.49		Moderate wet
> 0.49	0 ≤ SPI ≤ 0.99	> 40	Near normal
≤ -0.50	-0.99 ≤ SPI ≤ 0	≤ 40	Mild dry
≤ -1.0	-1.49 ≤ SPI ≤ -1	≤ 30	Moderate dry
≤ -2.0	-1.99 ≤ SPI ≤ -1.5	≤ 20	Severe dry
≤ -3	SPI ≤ -2	≤ 10	Extreme dry

4. Results

4.1 Temporal dynamics of rainfall anomalies

The Figure 2 illustrates the temporal variability of rainfall anomalies in Bundelkhand from 2000 to 2021 at two time scales SPI-3, and SPI-6, used for reflecting agricultural drought. The SPI-3 captures short term fluctuations and identifies frequent but brief drought events, whereas SPI-6 smooths these variations, revealing prolonged and more severe drought periods. Major drought episodes are evident in 2002, 2006, 2007, 2009, and 2015. In 2015, SPI-6 values ranges from -1.2 to -1.5, representing severe to extreme drought conditions. The six month, shows that in years 2007-2009 and 2014-2016 were dry periods for a long time which would have affected vegetation too (crop yields). Figure 3, the Rainfall Anomaly Index (RAI), also showed marked

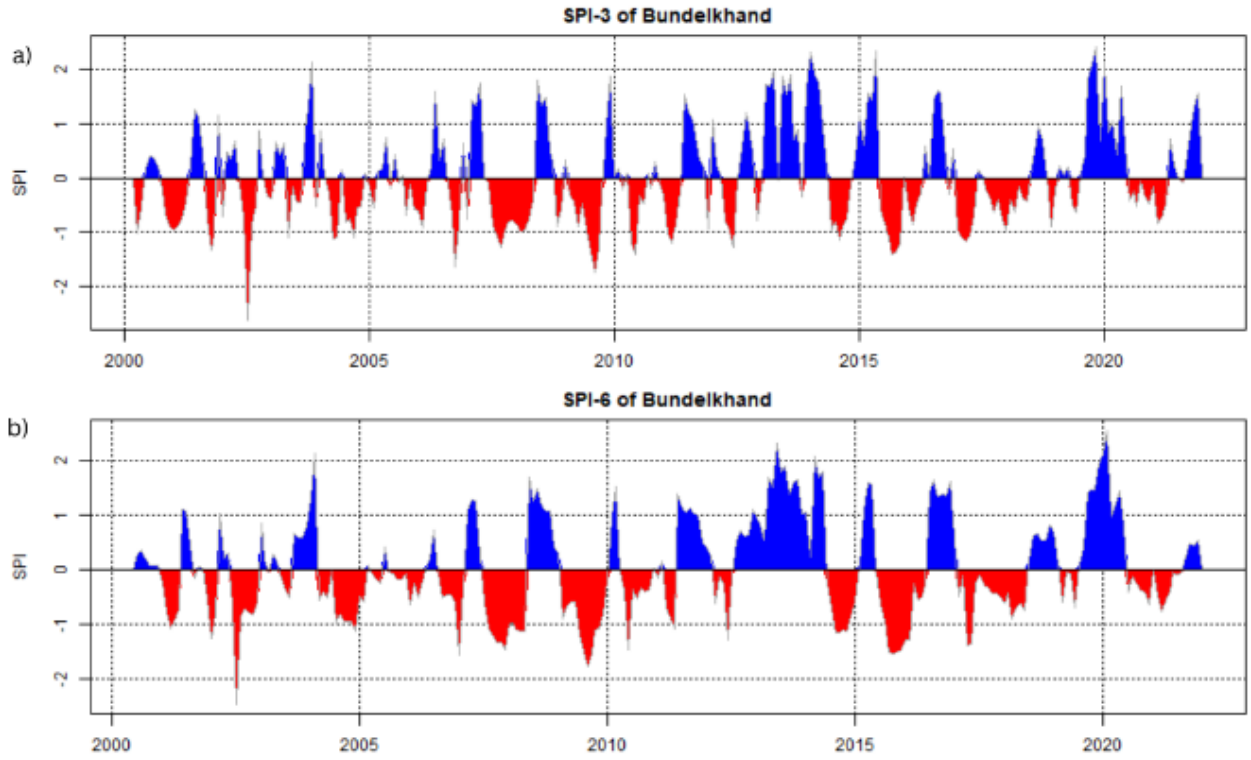

Figure 2. SPI plots for Bundelkhand at a) 3- and b) 6-month indicating red as drought and blue as normal periods.

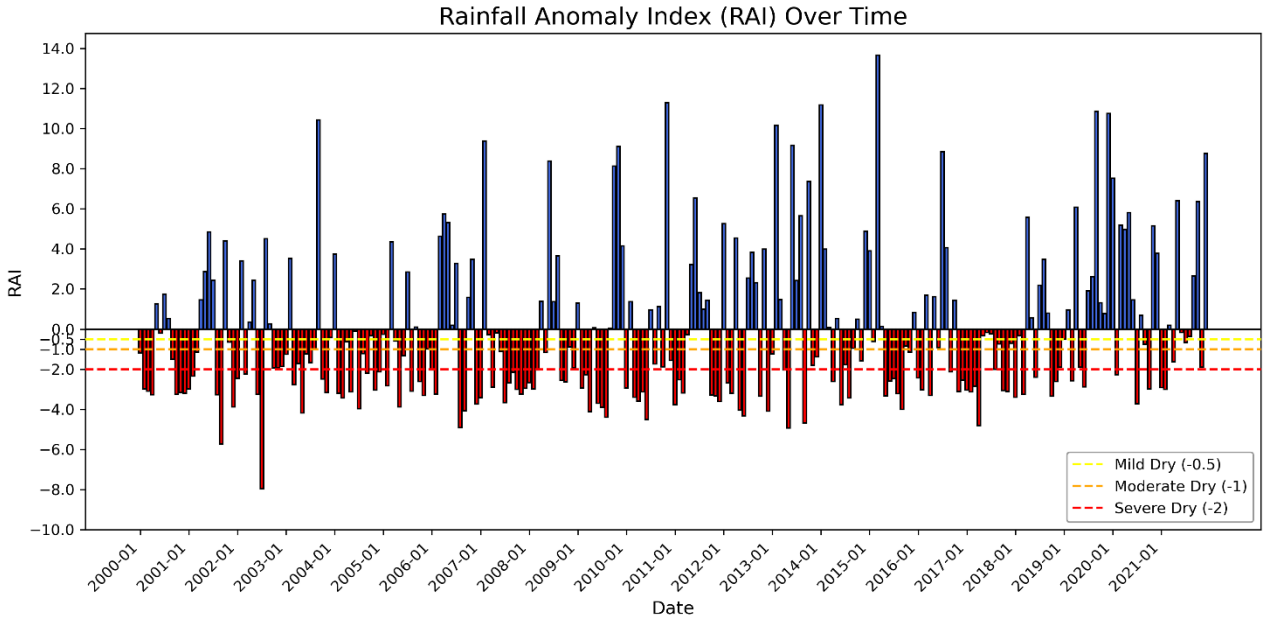

Figure 3. Rainfall Anomaly Index (RAI) plot. Normal conditions are above zero in blue and deficit is shown in red.

negative deviations during the same years indicating the drought periods. The RAI trends align closely with the SPI patterns, reinforcing the reliability of these indices in detecting rainfall deficits and drought intensity. Overall, the combined SPI and RAI analyses reveal that Bundelkhand experienced recurrent and intensifying dry spells during the study period, reflecting both short-term variability and long-term climatic stress on regional water availability and agriculture.

4.2 Spatial variations of soil and vegetation

Bundelkhand’s monsoon season extends from June to September, and the spatial distribution of the monthly SMCI and VCI for the drought year is shown in Figure 4. In June, soil moisture availability was notably low (Figure 4a), and vegetation exhibited mild to moderate drought conditions (Figure 4e). Vegetation stress intensified from July onward, progressing from mild to extreme drought across most areas except the eastern

This contribution has been peer-reviewed. The double-blind peer-review was conducted on the basis of the full paper.
https://doi.org/10.5194/isprs-annals-XI-3-2026-935-2026 | © Author(s) 2026. CC BY 4.0 License.

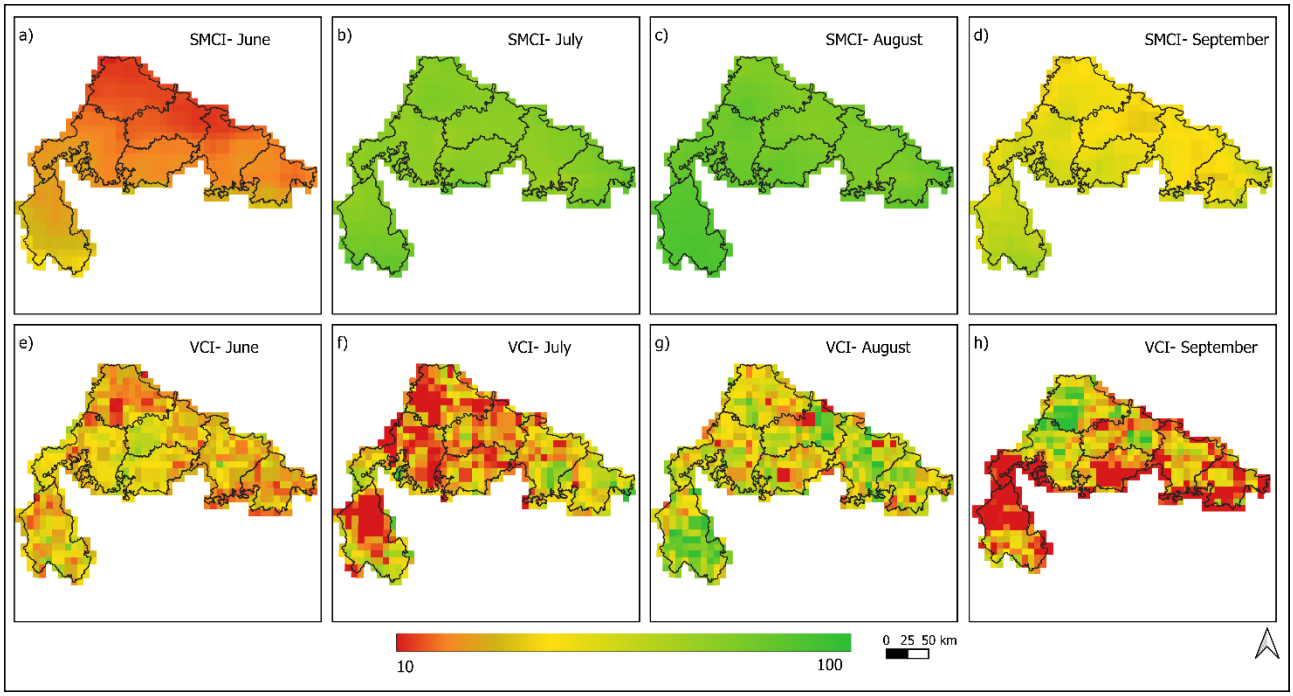

Figure 4. Spatial representation of VCI and SMCI for the monsoon month JJAS for drought year 2015. SMCI is from (a) to (d), and VCI from (e) to (h) for June, July, August, and September.

zone, where Banda and Chitrakoot remained under mild stress in July.

The soil moisture conditions normalized during July and August (Figure 4b-c) corresponding to the peak monsoon rainfall, while vegetation responded with a lag due to its slower recovery to precipitation changes. Consequently, VCI values improved in August (Figure 4g), indicating a temporary reduction in vegetation stress. However, in September, again SMCI and VCI reduction is seen (Figure 4d, 4h), directing to renewed vegetation stress (Figure 3h). During this time period, severe to extreme drought conditions was in the eastern and southern parts of the region, particularly in Banda, Chitrakoot, and Lalitpur districts. Here, SMCI and VCI patterns demonstrate a gradual spatial growth of drought in 2015 from early monsoon onset in June to increasing intensity by September.

4.3 Correlation between the indices

4.3.1 Correlation of rainfall, soil moisture and vegetation

Table 3 presents the Pearson correlation coefficients among the rainfall based indices (SPI, RAI), soil moisture (SMCI), and vegetation condition (VCI). All correlations are significant at 0.05 level. The highest correlation was observed between the SPI-3 and VCI, followed by SPI-6 and VCI. This indicates a strong linkage between short-to medium term rainfall variability and vegetation response. The correlation between SPI and SMCI was comparatively weaker, suggesting that soil moisture doesn’t responds directly to short-term variations. The RAI exhibited a moderate relationship with both SMCI and VCI. The vegetation response is always with a lag of certain time, and is visible from the correlation of SPI-3 and SPI-6 is better than SPI-1 and RAI.

Table 3. Correlation between different indices used in the study

Correlation	SMCI	VCI
SPI 1	0.274	0.306
SPI 3	0.249	0.492
SPI 6	0.184	0.491
RAI	0.296	0.303

4.3.2 Pixel wise correlation

Figure 5 shows the pixel wise correlation between SMCI and VCI for monsoon months (June- September). In June, (Figure 5a), higher correlations (0.4 - 0.6) are observed across the Bundelkhand, showing effective relation between soil moisture and vegetation response at the onset of monsoon. In contrast, July, August, and September (Figures 5b-d) most of the region shows a weak correlation at most regions with values ranging from (0.2 -0.4).

The yellow patches in the Figure 5 indicate moderate correlation, whereas red patches represent weak relationships. The regions of Jalaun, and Jhansi shows a very weak correlation during September. A monthly variability is observed in Lalitpur district throughout the season, showing dynamic interactions between soil and vegetation over time. The pattern of correlation is changing along the space and time in the monsoon month from June to September, showing the relation of soil water and vegetation dynamics. The mean SMCI-VCI correlation decreased from 0.519 in June to 0.367 in September indicating weakening soil-vegetation coupling as the monsoon progressed.

5. Discussions

The study examined the Bundelkhand region of Uttar Pradesh, which experienced several short-term droughts over the past 22 years. Regional rainfall has fluctuated considerably, with

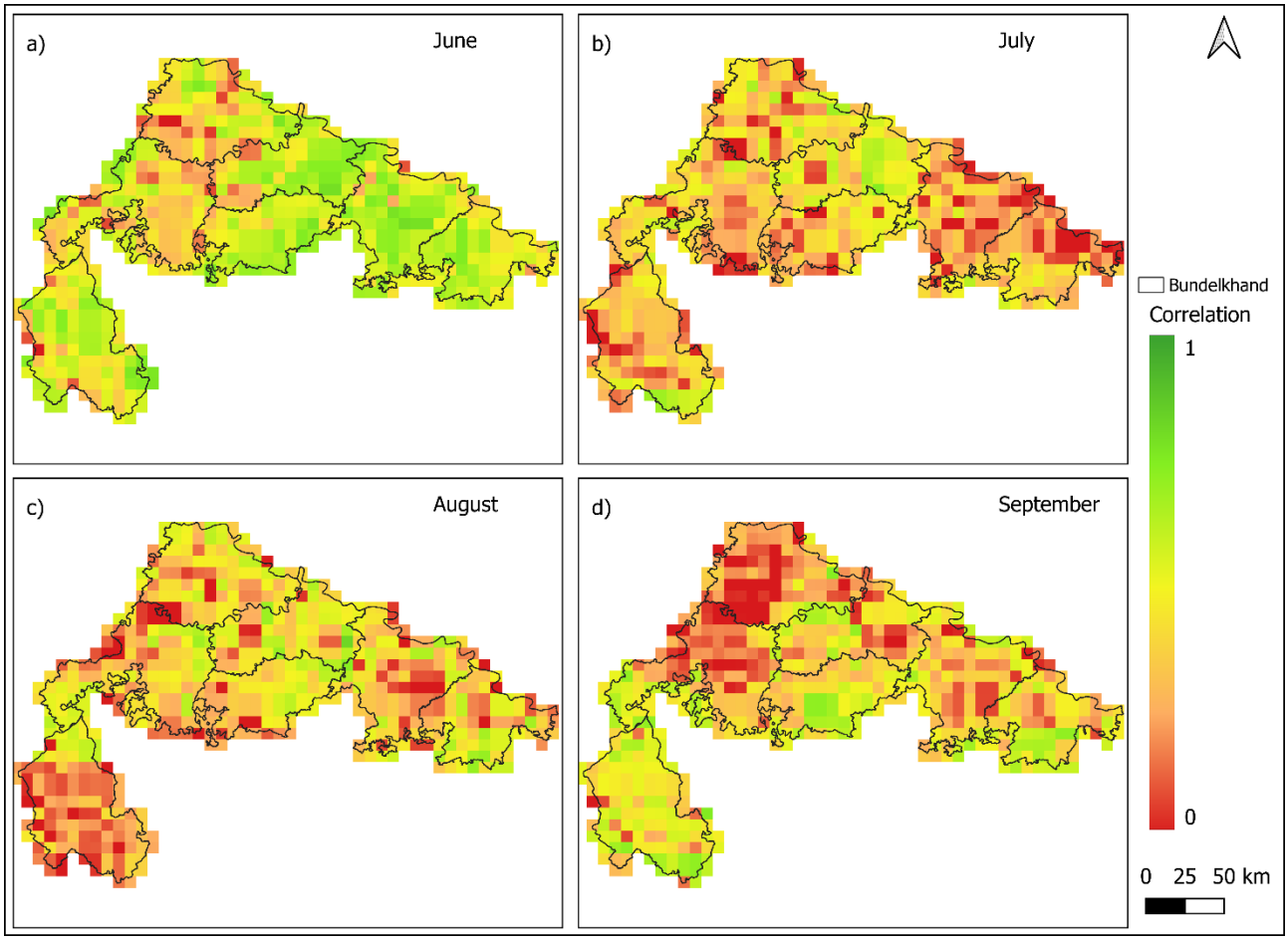

Figure 5. Pixel wise correlation between SMCI and VCI for monsoon months a) June, b) July, c) August and d) September

multiple episodes of severe and extreme deficits. As shown in (Figure 3), rainfall anomalies frequently fall below -2, indicating severe drought conditions. This event often persisted for consecutive months, such as from July 2007 to March 2008, or intensified rapidly over a short period, as in 2002, and 2015. Both years have been identified as major drought periods in earlier studies (V. Mishra et al., 2016; Pandey & Srivastava, 2018; Saharwardi et al., 2021; Uttar Pradesh Government, 2023).

The spatial distribution of agricultural drought, represented by VCI and the soil moisture availability as SMCI shown in Figure 4, shows that, in June, both indices indicate stressed conditions, as it is the onset of monsoon in India, but delayed up to mid to late June to reach Bundelkhand. This also coincides with the sowing period means no vegetation at present, explaining dry conditions observed during this month (Ahmed et al., 2019). With increased rainfall in July and August, soil moisture improves significantly, but vegetation shows a delayed recovery. The lagged vegetation response is evident in July when VCI values remain low despite rising SMCI values. By September, vegetation stress again intensifies, except north-western part including Jalaun, and Jhansi, exhibit relatively milder stress during the same period. However, the 8-km resolution may miss the droughts at specific region, as it covers a larger area.

Correlation analysis further supports these spatial observations. As presented in table 3, rainfall indices (SPI-3, SPI-6) show stronger correlations with VCI compared to SMCI, highlighting vegetation’s cumulative response to rainfall over short and medium term timescales (Javed et al., 2021; A. K. Mishra & Singh, 2010). The pixel wise correlation between SMCI and VCI (Figure 5) ranges from 0.25 to 0.7 across most areas, suggesting a moderate to strong linkage between soil moisture and vegetation condition during the monsoon months. This range is notably higher than correlations reported between VCI and the Standardized Precipitation Evapotranspiration Index (SPEI, also a rainfall and evapotranspiration based index) at different scales with VCI ranging from 0.11 to 0.20 (Liu et al., 2020). The future work will focus on inclusion of other variable such as temperature, evaporation, solar radiation, etc., analysing with multivariate drought indices as SPEI, and comparison with crop yield in the drought years, for better drought assessments.

6. Conclusions

The study focussed on understanding and analyzing the spatial and temporal dynamics of drought in the Bundelkhand region using multisource remote sensing data. Three key variables rainfall, soil moisture, and NDVI, were examined through multiple drought indices as SPI, RAI, SMCI, and VCI.

Rainfall, being the primary driver of drought, was first analyzed using SPI-3, and SPI-6 considering them as a indicator of agricultural drought. All indices recognized the drought periods as per literature, verifying their reliability for regional drought assessment. The 2015 drought year’s monsoon season SMCI and VCI indicated the onset of drought spatially. The indices showed

dry conditions in June, the start of monsoon, slowly recovering in July as soil moisture is increasing, but later falls towards the end of the season having vegetation stress. The patterns is observed in SPI and RAI too, for the same duration. Further, the correlation analysis proved that vegetation responds to rainfall with a temporal lag, as SPI-3, SPI-6, and VCI have high correlation (0.49) compared to SPI-1. Also, a declined mean correlation is observed from 0.519 to 0.367 from June to September, signifying that as moisture reduces, vegetation will also be affected.

The study confirms the use of remote sensing data and different index based analysis can capture drought onset, and its movement spatially and temporally. Such studies can be used in future to monitor droughts in data-sparse regions and provide necessary mitigation plans.

7. References

Ahmed, A., Deb, D., & Mondal, S. (2019). Assessment of rainfall variability and its impact on groundnut yield in Bundelkhand region of India. *Current Science*, *117*(5), 794–803. https://doi.org/10.18520/cs/v117/i5/794-803

Amrit, K., Pandey, R. P., & Mishra, S. K. (2018). Assessment of meteorological drought characteristics over Central India. *Sustainable Water Resources Management*, *4*(4), 999–1010. https://doi.org/10.1007/s40899-017-0205-5

Bhuiyan, C., Saha, A. K., Bandyopadhyay, N., & Kogan, F. N. (2017). Analyzing the impact of thermal stress on vegetation health and agricultural drought–a case study from Gujarat, India. *GIScience and Remote Sensing*, *54*(5), 678–699. https://doi.org/10.1080/15481603.2017.1309737

Chere, Z., & Debalke, D. B. (2024). Modeling agricultural drought based on the earth observation-derived standardized precipitation evapotranspiration index and vegetation health index in the northeastern highlands of Ethiopia. *Natural Hazards*, *120*(3), 3127–3151. https://doi.org/10.1007/s11069-023-06320-3

Dai, M., Huang, S., Huang, Q., Zheng, X., Su, X., Leng, G., Li, Z., Guo, Y., Fang, W., & Liu, Y. (2022). Propagation characteristics and mechanism from meteorological to agricultural drought in various seasons. *Journal of Hydrology*, *610*. https://doi.org/10.1016/j.jhydrol.2022.127897

Dikshit, A., & Pradhan, B. (2021). Interpretable and explainable AI (XAI) model for spatial drought prediction. *Science of the Total Environment*, *801*. https://doi.org/10.1016/j.scitotenv.2021.149797

Gond, S., Gupta, N., Patel, J., & Dikshit, P. K. S. (2023). Spatiotemporal evaluation of drought characteristics based on standard drought indices at various timescales over Uttar Pradesh, India. *Environmental Monitoring and Assessment*, *195*(3). https://doi.org/10.1007/s10661-023-10988-2

Gupta, A. kumar, Nair, S. S., Ghosh, O., Singh, A., & Dey, S. (2014). *Bundelkhand Drought*. 1–134.

Javed, T., Li, Y., Rashid, S., Li, F., Hu, Q., Feng, H., Chen, X., Ahmad, S., Liu, F., & Pulatov, B. (2021). Performance and relationship of four different agricultural drought indices for drought monitoring in China’s mainland using remote sensing data. *Science of the Total Environment*, *759*. https://doi.org/10.1016/j.scitotenv.2020.143530

Jiao, W., Tian, C., Chang, Q., Novick, K. A., & Wang, L. (2019). A new multi-sensor integrated index for drought monitoring. *Agricultural and Forest Meteorology*, *268*, 74–85. https://doi.org/10.1016/j.agrformet.2019.01.008

Karthikeyan, L., Chawla, I., & Mishra, A. K. (2020). A review of remote sensing applications in agriculture for food security: Crop growth and yield, irrigation, and crop losses. *Journal of Hydrology*, *586*. https://doi.org/10.1016/j.jhydrol.2020.124905

Kogan, F. N. (1995). Application of vegetation index and brightness temperature for drought detection. *Advances in Space Research*, *15*(11), 91–100. https://doi.org/10.1016/0273-1177(95)00079-T

Kraus, E. B. (1977). Subtropical Droughts and Cross-Equatorial Energy Transports. *Monthly Weather Review*, *105*(8), 1009–1018. https://doi.org/https://doi.org/10.1175/1520-0493(1977)105<1009:SDACEE>2.0.CO;2

Li, M., Cao, S., Zhu, Z., Wang, Z., Myneni, R. B., & Piao, S. (2023). Spatiotemporally consistent global dataset of the GIMMS Normalized Difference Vegetation Index (PKU GIMMS NDVI) from 1982 to 2022. *Earth System Science Data*, *15*(9), 4181–4203. https://doi.org/10.5194/essd-15-4181-2023

Liu, Q., Zhang, S., Zhang, H., Bai, Y., & Zhang, J. (2020). Monitoring drought using composite drought indices based on remote sensing. *Science of the Total Environment*, *711*. https://doi.org/10.1016/j.scitotenv.2019.134585

Lu, Y., Yang, T., Fu, J., & Song, W. (2025). Utility of the standardized precipitation evapotranspiration index (SPEI) to detect agricultural droughts over China. *Journal of Hydrology: Regional Studies*, *58*, 102190. https://doi.org/10.1016/J.EJRH.2025.102190

Mahmoudi, P., Rigi, A., & Miri Kamak, M. (2019). Evaluating the sensitivity of precipitation-based drought indices to different lengths of record. *Journal of Hydrology*, *579*. https://doi.org/10.1016/j.jhydrol.2019.124181

Mckee, T. B., Doesken, N. J., & Kleist, J. (1993). THE RELATIONSHIP OF DROUGHT FREQUENCY AND DURATION TO TIME SCALES. In *Eighth Conference on Applied Climatology*.

Ministry of Agriculture and Farmers Welfare, & Government of India. (2022). *National Crisis Management Plan for Drought*.

Mishra, A. K., & Singh, V. P. (2010). A review of drought concepts. In *Journal of Hydrology* (Vol. 391, Numbers 1–2, pp. 202–216). https://doi.org/10.1016/j.jhydrol.2010.07.012

Mishra, V., Aadhar, S., Asoka, A., Pai, S., & Kumar, R. (2016). On the frequency of the 2015 monsoon season drought in the Indo-Gangetic Plain. *Geophysical Research Letters*, *43*(23), 12,102-12,112. https://doi.org/10.1002/2016GL071407

Mukhawana, M. B., Kanyerere, T., Kahler, D., Masilela, N. S., Lalumbe, L., & Umunezero, A. A. (2024). Hydrological drought assessment using the standardized groundwater index and the standardized precipitation index in the Berg River Catchment, South Africa. *Journal of Hydrology: Regional Studies*, *53*. https://doi.org/10.1016/j.ejrh.2024.101779

Ocampo-Marulanda, C., Fernández-Álvarez, C., Cerón, W. L., Canchala, T., Carvajal-Escobar, Y., & Alfonso-Morales, W. (2022). A spatiotemporal assessment of the high-resolution CHIRPS rainfall dataset in southwestern Colombia using combined principal component analysis. *Ain Shams Engineering Journal*, *13*(5). https://doi.org/10.1016/J.ASEJ.2022.101739

Palmer. (1965). *Meteorological Drought*.

Pandey, V., & Srivastava, P. K. (2018). INTEGRATION OF SATELLITE, GLOBAL REANALYSIS DATA AND MACROSCALE HYDROLOGICAL MODEL FOR DROUGHT ASSESSMENT IN SUB-TROPICAL REGION OF INDIA. *The International Archives of the Photogrammetry, Remote Sensing and Spatial Information Sciences*, *XLII–3*(3), 1347–1351. https://doi.org/10.5194/ISPRS-ARCHIVES-XLII-3-1347-2018

Pandey, V., Srivastava, P. K., Singh, S. K., Petropoulos, G. P., & Mall, R. K. (2021). Drought identification and trend analysis using long-term chirps satellite precipitation product in bundelkhand, india. *Sustainability (Switzerland)*, *13*(3), 1–20. https://doi.org/10.3390/su13031042

Prakash, S. (2019). Performance assessment of CHIRPS, MSWEP, SM2RAIN-CCI, and TMPA precipitation products across India. *Journal of Hydrology*, *571*, 50–59. https://doi.org/10.1016/J.JHYDROL.2019.01.036

Saharwardi, M. S., Mahadeo, A. S., & Kumar, P. (2021). Understanding drought dynamics and variability over Bundelkhand region. *Journal of Earth System Science*, *130*(3). https://doi.org/10.1007/s12040-021-01616-z

Satapathy, T., Dietrich, J., & Ramadas, M. (2024). Agricultural drought monitoring and early warning at the regional scale using a remote sensing-based combined index. *Environmental Monitoring and Assessment 2024 196:11*, *196*(11), 1–27. https://doi.org/10.1007/S10661-024-13265-Y

Thomas, T., Nayak, P. C., & Ghosh, N. C. (2015). Spatiotemporal Analysis of Drought Characteristics in the Bundelkhand Region of Central India using the Standardized Precipitation Index. *Journal of Hydrologic Engineering*, *20*(11), 05015004. https://doi.org/10.1061/(asce)he.1943-5584.0001189

Uttar Pradesh Government. (2023). *Uttar Pradesh: State Disaster Management Plan-2023 (Part-1)*. https://upsdma.up.nic.in/2023/SDMP-Plan-Part-1.pdf

Van Rooy, M. P. (1965). *A rainfall anomally index independent of time and space, notos*. 43–48.

Vicente-Serrano, S. M., Beguería, S., & López-Moreno, J. I. (2010). A multiscalar drought index sensitive to global warming: The standardized precipitation evapotranspiration index. *Journal of Climate*, *23*(7), 1696–1718. https://doi.org/10.1175/2009JCLI2909.1

Vicente-Serrano, S. M., Domínguez-Castro, F., Reig, F., Tomas-Burguera, M., Peña-Angulo, D., Latorre, B., Beguería, S., Rabanaque, I., Noguera, I., Lorenzo-Lacruz, J., & El Kenawy, A. (2023). A global drought monitoring system and dataset based on ERA5 reanalysis: A focus on crop-growing regions. *Geoscience Data Journal*, *10*(4), 505–518. https://doi.org/10.1002/gdj3.178

Werick, W. J. , Willeke, G. E. , Guttman, N. B. , Hosking, J. R. M. , & Wallis, J. R. (1994). National Drought Atlas Developed. *Eos*, *75*(8), 89–90. https://doi.org/10.1029/94eo00706

Zhang, L., Jiao, W., Zhang, H., Huang, C., & Tong, Q. (2017). Studying drought phenomena in the Continental United States in 2011 and 2012 using various drought indices. *Remote Sensing of Environment*, *190*, 96–106. https://doi.org/10.1016/j.rse.2016.12.010

Zhao, X., Xia, H., Pan, L., Song, H., Niu, W., Wang, R., Li, R., Bian, X., Guo, Y., & Qin, Y. (2021). Drought Monitoring over Yellow River Basin from 2003–2019 Using Reconstructed MODIS Land Surface Temperature in Google Earth Engine. *Remote Sensing 2021, Vol. 13, Page 3748*, *13*(18), 3748. https://doi.org/10.3390/RS13183748